A FAST VISCOUS CORRECTION METHOD APPLIED TO SMALL DISTURBANCE POTENTIAL TRANSONIC FLOWS IN THE FREQUENCY DOMAIN

Paulo C. Greco Jr.*, Lee Y. Sheng*
***University of Sao Paulo – Brazil**

Keywords: *Transonic Flow, TSD Equation, Frequency Domain, Viscous Correction*

Abstract

A fast viscous correction method is applied to the solution of the transonic small disturbance potential equations in the frequency domain. The objective is to improve transonic results for which shock/boundary-layer interaction is important. That method has been applied to time domain analyses in the past with good results. In frequency domain the spatial nonlinear terms are preserved using a transformation technique known as harmonic averaging. The main reason for using the TSD equation still is computational cost, especially when dealing with complete aircraft configurations. Obtained results compare well with published experimental data for steady transonic pressure distribution and flutter analysis at low mean angles of attack.

1 Introduction

The computational cost associated with the aeroelastic analysis of complete aircraft configurations in transonic flow can be very high, depending on the aerodynamic equations being solved. In view of that, working with the transonic small disturbance (TSD) equation can still be quite attractive considering that the results can be realistic when dealing with aeroelastic problems such as flutter at low angles of attack, for instance. In general, cases where flow separation is not expected and drag estimation is not required can be adequately treated using the TSD equation. Corrections for entropy and vorticity effects can be introduced improving the results for shock location and strength. Shock/boundary-layer corrections have also been introduced in the past, improving results for cases where thickening of the boundary-layer behind the shock alters significantly its position and intensity. Such an effect can play an important role in the occurrence of limit cycle oscillations.

Frequency domain analysis of flutter can have significant advantages over time domain analysis. Restrictions on time step size and the required total time to characterize typical flutter frequencies [5] can impose greater computational costs than equivalent frequency domain analysis which is free of those restrictions. On the other hand, frequency domain analysis is often criticized for requiring linearization of the equations. There are a few techniques which allow transformation into the frequency domain while maintaining the non-linear spatial terms. The harmonic averaging technique [6] maintains the non-linear spatial terms but assumes harmonic variation of all time dependent variables.

According to Holst [4] the existing codes based on the potential equation (both the full and the small disturbance) are mature enough to be used in routine unsteady transonic flow analysis for aircraft development. The present paper describes work being conducted on the introduction of corrections for shock/boundary-layer interaction in transonic flutter analysis in the frequency domain. The corrections are introduced in an unsteady transonic small disturbance computer code named UsTSD [1].

2 Methodology

2.1 TSD Equation in the Frequency Domain

The conservative-form, non-dimensional, TSD equation may be written as

$$\begin{aligned}&(A\phi_t + B\phi_x)_t = \\ &(E\phi_x + F\phi_x^2 + G\phi_y^2)_x + \\ &(\phi_y + H\phi_x\phi_y)_y + (\phi_z)_z\end{aligned} \tag{1}$$

where

$$\begin{aligned}A &= k^2 M_\infty^2, \\ B &= 2k M_\infty^2, \\ E &= 1 - M_\infty^2, \\ F &= -\frac{\gamma+1}{2} M_\infty^{1.75}, \\ G &= \frac{\gamma-1}{2} M_\infty^2, \\ H &= (1-\gamma) M_\infty^2,\end{aligned} \tag{2}$$

ϕ is the non-dimensional perturbation velocity potential and M_∞ is the free stream Mach number. Harmonic averaging is used to convert the TSD equation into the frequency domain [1]. The perturbation velocity potential is split into a steady and an unsteady component as

$$\phi = \phi^s + \phi^u \cos(\theta + \delta) \tag{3}$$

where ϕ^s is the steady component, ϕ^u is the unsteady component, θ is the phase angle of the harmonic structural motion and δ is the phase angle between structural motion and aerodynamic forces.

The transformation yields three equations: the steady state equation

$$\begin{aligned}&[E\phi_x^s + F(\phi_x^s)^2 + G(\phi_y^s)^2]_x + \\ &(\phi_y^s + H\phi_x^s\phi_y^s)_y + (\phi_z^s)_z = 0,\end{aligned} \tag{4}$$

the in-phase equation

$$\begin{aligned}&A\phi^{u(i)} + B\phi^{u(o)} + \\ &[E\phi_x^{(i)} + F(\phi_x^{(i)})^2 + G(\phi_y^{(i)})^2]_x + \\ &(\phi_y^{(i)} + H\phi_x^{(i)}\phi_y^{(i)})_y + (\phi_z^{(i)})_z = 0,\end{aligned} \tag{5}$$

and the out-of-phase equation

$$\begin{aligned}&A\phi^{u(o)} - B\phi^{u(i)} + \\ &[E\phi_x^{(o)} + F(\phi_x^{(o)})^2 + G(\phi_y^{(o)})^2]_x + \\ &(\phi_y^{(o)} + H\phi_x^{(o)}\phi_y^{(o)})_y + (\phi_z^{(o)})_z = 0,\end{aligned} \tag{6}$$

where

$$\begin{aligned}\phi^{(i)} &= \phi^s + \phi^{u(i)}, \\ \phi^{(o)} &= \phi^s + \phi^{u(o)}, \\ \phi^{u(i)} &= \phi^u \cos\delta, \\ \phi^{u(o)} &= \phi^u \sin\delta.\end{aligned} \tag{7}$$

Boundary conditions are also transformed using harmonic averaging. The equations are rewritten using first order finite difference approximations. Corrections for entropy and vorticity effects are introduced [2]. Central differences are used in subsonic regions while upstream differences (x direction) are used in supersonic regions. The domain is discretized by fine regular grids embedded in a coarse grid (each surface has its own fine grid). Linear transformations are used to make the lifting surfaces rectangular. Fuselage-like bodies are represented by boxes. The system of equations is solved using the SLOR technique. The steady equation is solved first and the in-phase and out-of-phase equations are solved simultaneously.

2.2 A Fast Viscous Correction Method

The fast viscous correction method is described by Lee [3]. That is a semi-empirical method in which the thickening of the boundary-layer behind the shock can be modeled by an equivalent vertical velocity:

$$\nu(s) = \beta M\,(w + \delta^*) \tag{8}$$

where s is a chordwise coordinate, β is an empirical constant (equal to 2 for unsteady

small-disturbance flows), M is the local Mach number, δ^* is the local boundary-layer displacement thickness and w models a "viscous wedge" representing the boundary-layer thickening behind the shock. The boundary-layer displacement thickness is neglected. The "viscous wedge" is null upstream of the shock locations and downstream of the shock it is expressed as

$$w = \beta_1 \theta_{max} \left[1 - \exp\left(\frac{s_{sh} - s}{c} \beta_1 \right) \right] \qquad (9)$$

where β_1 is an empirical constant (normally equal to 0.1), θ_{max} is the maximum flow deflection angle across the shock, s_{sh} is the chordwise shock location and c is the local lifting surface chord.

The method is implemented through a modification of the surface boundary-layer admitting the existence of transpiration. The lifting surface boundary conditions are given by (steady, in-phase and out-of-phase)

$$\phi_z^s = \frac{1}{M^{.25}} \left(\frac{\partial}{\partial x} f^s - \alpha_s \right) \qquad (10)$$

$$\phi_z^i = \frac{1}{M^{.25}} \left(\frac{\partial}{\partial x} f^s - \frac{\partial}{\partial x} f^v - \alpha_s \right) \qquad (11)$$

$$\phi_z^o = \frac{1}{M^{.25}} \left(\frac{\partial}{\partial x} f^s - k \frac{\partial}{\partial x} f^v - \alpha_s \right) \qquad (12)$$

where α_s is the steady (or mean) angle of attack, f^s is the airfoil section shape, f^v is the airfoil section local vertical velocity and k is the reduced frequency. The "viscous wedge" can either be introduced directly in f^s or introduced in f^v through Eq. (8).

3 Results

3.1 RAE2822 Airfoil Section

The supercritical RAE2822 airfoil section is used as a benchmark for computational transonic flow analysis [7]. Only the steady pressure distribution results are compared to the experimental data. The objective is to compare shock strength and position with and without viscous correction. Fig. 1 shows the pressure coefficient distribution for Mach 0.729 and angle of attack of 2.31° using a fully conservative differencing scheme.

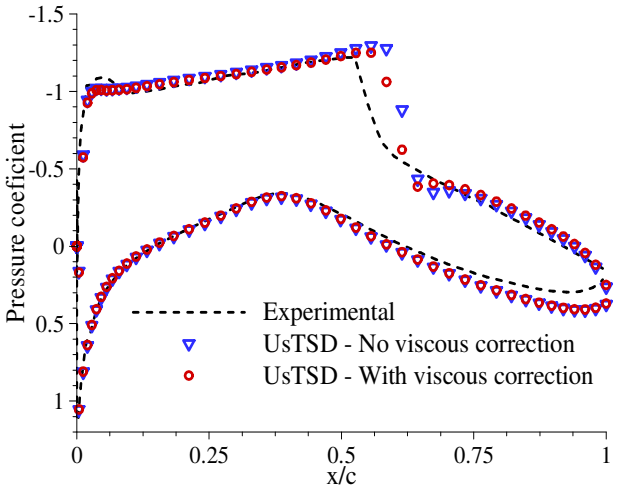

Fig. 1. Pressure coefficient distribution for the RAE2822 airfoil section at $M = 0.729$ and $\alpha = 2.31°$ with conservative differencing

The use of viscous correction moves the shock upstream and reduces its strength. That is the expected behavior caused by the boundary-layer thickening behind the shock. The correction is not strong enough to move the shock to the same position as for the experimental data.

Fig. 2 shows the pressure coefficient distribution at the same flow conditions but now using a non-conservative differencing scheme. It is well known that, in general, the use of non-conservative differencing produces results which are closer to experimental data than those obtained using conservative differencing. The results in Fig. 2 show exactly that with shock position and strength much closer to the experimental data than before. Again the use of viscous correction moves the shock slightly forward this time almost coinciding with the experimental data. Fig. 3 shows in detail the differences in shock position for calculations with and without viscous correction.

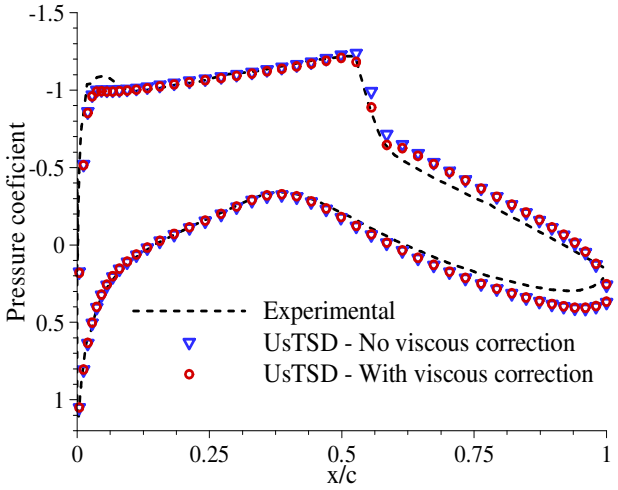

Fig. 2. Pressure coefficient distribution for the RAE2822 airfoil section at $M = 0.729$ and $\alpha = 2.31^{o}$ with non-conservative differencing.

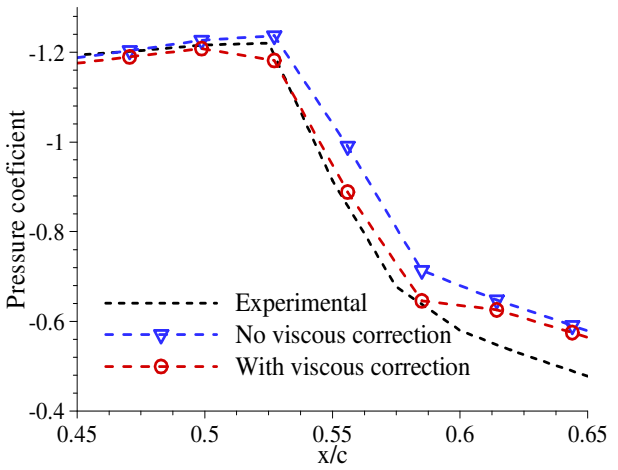

Fig. 3. Detail of shock location for the RAE2822 airfoil section at $M = 0.729$ and $\alpha = 2.31^{o}$ with non-conservative differencing.

The effect of viscous correction is much more subtle than that of using conservative or non-conservative differencing.

3.2 NACA0012 Airfoil Section

Numerical results for a NACA0012 airfoil section are presented in Reference [2]. Those results where obtained using the computer code FLO52 which solves the Euler equations. Again the objective is to compare results for shock strength and position. The pressure coefficient distribution is shown in Fig. 4 for Mach 0.8 and angle of attack of 1.25^{o} using a fully conservative differencing scheme.

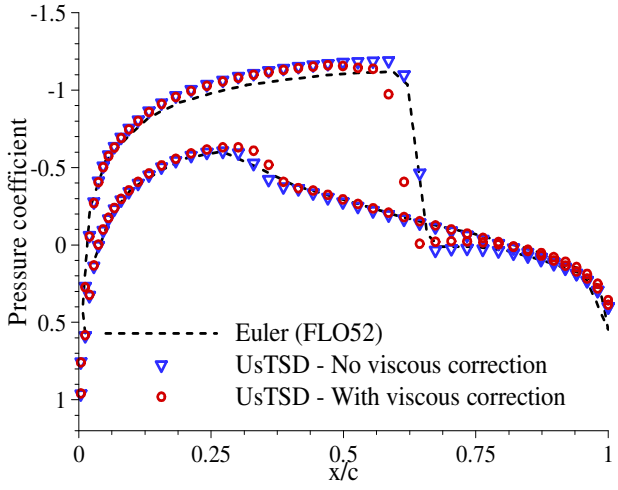

Fig. 4. Pressure coefficient distribution for the NACA0012 airfoil section at $M = 0.8$ and $\alpha = 1.25^{o}$ with conservative differencing.

The results obtained with no viscous correction are closer to the FLO52 results than those obtained with the correction. This is expected since FLO52 is an inviscid code. The effect of viscous correction again shows the correct trend with the shock moving upstream due to the thickening of the boundary layer. The effect of the viscous correction is more evident than that for the RAE2882 section.

Fig. 5 shows the pressure coefficient distribution for the NACA 0012 airfoil section at the same flow conditions.

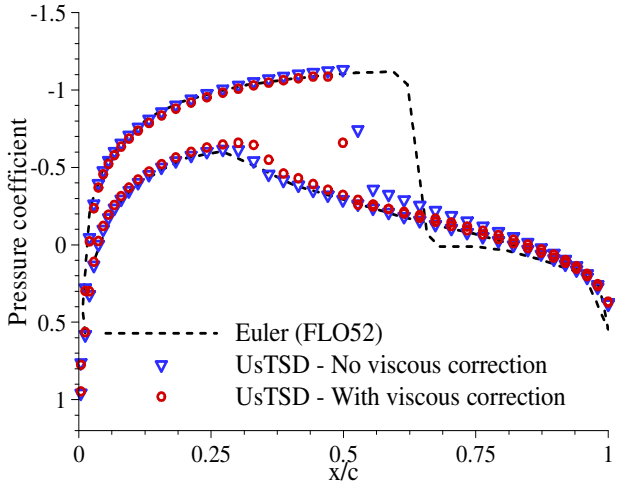

Fig. 5. Pressure coefficient distribution for the NACA0012 airfoil section at $M = 0.8$ and $\alpha = 1.25^{o}$ with non-conservative differencing.

The results for shock position and strength are very different than the FLO52 results. This is expected since FLO52 uses fully conservative

differencing. The viscous correction moves the shock upstream.

3.3 NLR7301 Airfoil Section

Experimental results for the NLR7301 airfoil section are presented by Tang et.al. [8]. The flow conditions involve some shock induced separation. The objective is to assess the degree of viscous correction obtained for such a case. Fig. 6 shows the pressure coefficient distribution for Mach 0.753 and angle of attack of -0.08° using non-conservative differencing.

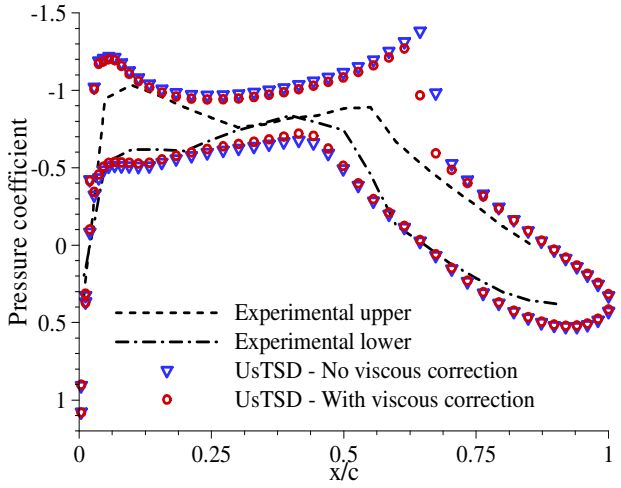

Fig. 6. Pressure coefficient distribution for the NLR7301 airfoil section at $M = 0.753$ and $\alpha = -0.08^{o}$ with non-conservative differencing.

The viscous correction is not effective enough to approximate experimental and numerical results even when non-conservative differencing is used. This is a case for which the TSD formulation may be inadequate even though the angle of attack is very small.

3.4 AGARD I-Wing 445.6 Flutter Analysis

The flutter analysis for the I-Wing 445.6 [9] was conducted to assess the effect of the viscous correction on the results. The wing flexible structure is represented by five normal modes with their natural frequencies and generalized masses. Analysis of the viscous correction effect was restricted to Mach 0.96 which is right in the transonic dip of the flutter curve. Fig. 7 shows the flutter results for the I-445.6 wing obtained with the computer code UsTSD with conservative differencing and without viscous correction. Details on the calculation of the flutter results can be found in Ref. [1].

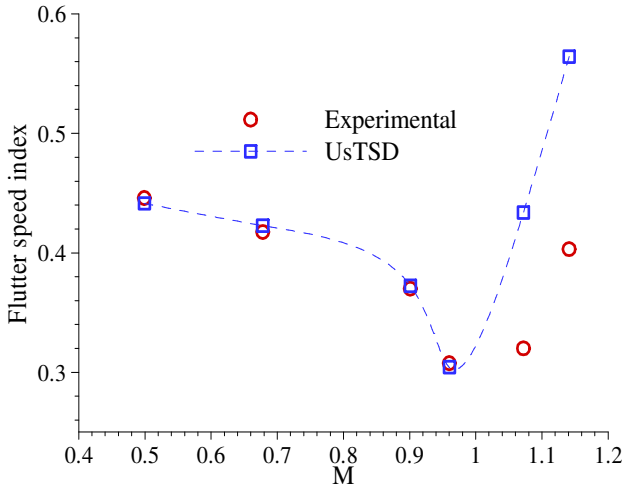

Fig. 7. Flutter speed index for the I-445.6 wing with conservative differencing.

The large difference in the supersonic range may be due to experimental procedure errors rather than computational problems. The analysis at Mach 0.96 was conducted with four different options. The results are presented on Table 1.

Table 1: Comparison of flutter results for the I-445.6 wing at Mach 0.96.

Case	Flutter Speed Index	Flutter Frequency (Hz)
Conservative No viscous correction	0.304	13.4
Conservative With viscous correction	0.300	13.3
Non-conservative No viscous correction	0.320	13.9
Non-conservative With viscous correction	0.322	13.9

The experimental results for Mach 0.96 are a flutter speed index of 0.308 and a flutter frequency of 13.9 Hz. The results are too close to each other to be distinguishable in a graph such as Fig. 6. It can be seen, however, that the closest result for flutter speed index is that for conservative differencing with no viscous

correction. The closest results for flutter frequency are those for non-conservative differencing.

4 Conclusions

The steady flow results show that the viscous correction is having the desired qualitative effect. The quantitative effect is more or less pronounced depending on the test case. The results for the NLR7301 airfoil section are very different from the experimental results indicating that, for that case, the TSD equation with the present corrections may be inadequate. More cases need to be investigated to better develop the computer code.

The flutter results show virtually no influence of the viscous correction on the flutter speed index or the flutter frequency. It appears that the I-445.6 wing flutter case is adequately modeled by the inviscid aerodynamic model, except in the supersonic range, where experimental errors may have affected the results.

5 Acknowledgments

The computer code UsTSD, which is used as a basis for the present work, was developed at the University of Kansas under the supervision of Dr. Edward Lan.

The present work is being partially financed by FAPESP of Brazil.

6 References

[1] Greco Jr. P, Lan C and Lim T. Frequency domain unsteady transonic aerodynamics for flutter and limit cycle oscillation prediction. *35th AIAA Aerospace Sciences Meeting and Exhibit*, Reno, NV, U.S.A., Paper No. 97-0835, January 1997.

[2] Batina J. Unsteady Transonic Small-Disturbance Theory Including Entropy and Vorticity Effects. *Journal of Aircraft*, Vol. 26, No. 6, pp 531-538, June 1989.

[3] Lee S. A fast viscous correction method for transonic aerodynamics. *Computational Methods in Viscous Aerodynamics*, Chapter 10, T.K.S. Murthy and C.A. Brebbia editors, Elsevier, 1990.

[4] Holst T. Transonic flow computations using nonlinear potential methods. *Progress in Aerospace Sciences*, No. 36, pp.1-61, 2000.

[5] Bennett R and Batina J. Wing-flutter calculations with the CAP-TSD unsteady transonic small-disturbance program. *Journal of Aircraft*, Vol. 26, No. 9, pp 876-882, September 1989.

[6] Nayfeh A and Mook D. *Nonlinear Oscillations*. John Wiley & Sons, 1979.

[7] Cook P, McDonald M and Firmin M. Aerofoil RAE 2822 - pressure distributions, and boundary layer and wake measurements. *Experimental Data Base for Computer Program Assessment*, AGARD Report AR 138, 1979.

[8] Tang L, Bartels R, Chen P and Liu D. Numerical investigation of transonic limit cycle oscillations of a two-dimensional supercritical wing. *Journal of Fluids and Structures*, No.17, pp 29–41, 2003.

[9] Yates Jr. E, Land N and Foughner J. Measured and calculated subsonic and transonic flutter characteristics of a 45^{o} sweptback wing planform in air and in freon-12 in the Langley Transonic Dynamics Tunnel. *NASA TN-1616*, 1963.